

A facile preparation of NiO/Ni composites as high-performance pseudocapacitor materials

Cite this: *RSC Advances*, 2013, 3, 8003

Miaomiao Liu, Jie Chang, Jing Sun* and Lian Gao

We report a facile way to prepare NiO/Ni composites with a positive on their specific capacitances as supercapacitor electrodes. Various NiO/Ni composites were obtained by controlling the reduction time of NiO by H₂. The morphology of the products was characterized by transmission electron microscopy (TEM) and scanning electron microscopy (SEM). The electrochemical performance of electrodes was investigated by cyclic voltammetry (CV) and the galvanostatic charge/discharge test. The results of electrochemical tests show that the as-prepared NiO and NiO/Ni all reveal stable cycling performance and remarkable rate performance. The resulting NiO/Ni40, obtained by calcining NiO in H₂ for 40 min, could achieve a high specific capacitance of 760 F g⁻¹ at 20 A g⁻¹, significantly higher than the 480 F g⁻¹ found for NiO. Additionally, the specific capacitance of NiO/Ni40 remained as high as 816 F g⁻¹ after a 1000-cycle test at 4 A g⁻¹, revealing superb electrochemical characteristics. This study provides a viewpoint that the introduction of an appropriate amount of Ni particles could enhance the specific capacitance of NiO as a supercapacitor electrode.

Received 12th December 2012,
Accepted 18th March 2013

DOI: 10.1039/c3ra23286g

www.rsc.org/advances

1. Introduction

Nowadays, more and more attention has been paid to various power source devices for clean and efficient energy storage, such as Li-ion batteries, supercapacitors, fuel cells and so on.^{1–5} Among them, supercapacitors show promise by virtue of their high power density, fast charge/discharge capability, and long life cycle. However, the relatively low energy density of traditional electrical double layer capacitors (EDLCs) limits their application as a power supply.^{6,7} Therefore, recent research has focused on pseudocapacitor materials, such as RuO₂,⁸ NiO,^{9–13} Ni(OH)₂,^{14–17} Co₃O₄,¹⁸ MnO₂,^{19,20} and NiCo₂O₄.²¹ They show high specific capacitance and energy density, which ascribe to Faradic redox reactions. Nevertheless, their poor electrical conductivity leads to slower electron transport rates. Less active material availability, further impairs their electrochemical performance. In order to solve this issue, recently a number of efforts have focused on improving the electrical conductivity. Of all the strategies, two methods are used widely. One is that materials with high pseudocapacitance are incorporated directly into conductive carbon materials, such as activated carbon,²² mesoporous carbon,²³ carbon nanotubes,^{24,25} or graphene.^{15,26} However, some functional groups are generally introduced onto the carbon materials for better bonding with the pseudocapacitor materials, which always results in a decrease in conductivity of the carbon materials.

The other method is to construct a pseudocapacitor material–conductive matrix hybrid nanostructure.^{27–32} The matrix with a porous conductive network improves the electron transport rate leading to an enhanced supercapacitor performance. For example, Chen *et al.*²⁷ synthesized a MnO₂–gold matrix hybrid structure as a supercapacitor. The nanoporous gold matrix enhanced conductivity, making the MnO₂ achieve a high specific capacitance of 1145 F g⁻¹. Xiao *et al.*²⁸ constructed monolithic NiO–Ni matrix composites as supercapacitors by mechanically compacting Ni powder to produce thin pellet disks, followed by a subsequent low-temperature annealing process. The NiO–Ni matrix electrode possessed a maximum specific capacitance of 910 F g⁻¹. Though the pseudocapacitor material–conductive matrix hybrid nanostructures can improve the performance of supercapacitors significantly, the preparation processes above are high-cost or not easy to control. Thus, it is a major topic of interest to find a new way to increase the electrical conductivity. A key to achieve this aim is to build a type of material in which the distributions of pseudocapacitive and conductive materials are homogeneous and a fast ion and electron transfer will be guaranteed.

We constructed a binary system composed of Ni and NiO by a simple reduction method. This unique design has the following merits. NiO, serving as the active material in the NiO/Ni composite, has exhibited a great electrochemical performance because of its higher surface area and good charge storage properties. Meanwhile, the conductive particles of Ni provide facile electron transport paths for fast Faradic reaction and further improve the availability of NiO. The coexistence of Ni and NiO synergistically, influences the

The State Key Lab of High Performance Ceramics and Superfine Microstructure, Shanghai Institute of Ceramics, Chinese Academy of Sciences, 1295 Dingxi Road, Shanghai 200050, P. R. China. E-mail: jingsun@mail.sic.ac.cn; Fax: +86-21-52413122; Tel: +86-21-52414301

capacitance values. As a consequence, Ni obtained by a reduction method could improve the conductivity of NiO/Ni composites, thus enhancing their electrochemical characteristics and potential applications. This work used a simple way to prepare a NiO/Ni composite as an electrode material and could control the ratio of NiO and Ni conveniently. Although NiO/Ni systems as supercapacitors have been reported previously, the electrodes were prepared by constructing a self-supporting structure.^{28,33,34} We however, prepared the NiO/Ni electrodes by the traditional slurry method and the specific capacitance of the electrodes was better than that of similar systems reported previously based on the total mass of NiO and Ni.^{28,33} NiO/Ni electrodes by the traditional slurry method are used as supercapacitors for the first time in this work. Therefore, this study presents the new idea that introducing an appropriate amount of metal to an active material can enhance the electrochemical performance of supercapacitor electrodes.

2. Experimental

2.1 Materials

$\text{Ni}(\text{NO}_3)_2 \cdot 6\text{H}_2\text{O}$ and *N*-methyl pyrrolidone (NMP) were purchased from Sinopharm Chemical Reagent Co., Ltd., China, in analytical purity and used without further purification. Deionized water was used throughout the experiments.

2.2 Preparation of samples

NiO was prepared by a previously reported method.³⁵ In a typical synthesis, 8 g of $\text{Ni}(\text{NO}_3)_2 \cdot 6\text{H}_2\text{O}$ was dissolved in 200 mL of a mixed solvent of NMP/ H_2O (volume ratio 39 : 1). The solution was kept stirring at 190 °C for 2 h. Then the suspension was transferred to a Teflon-lined autoclave for hydrothermal reaction at 190 °C for 6 h. The product was filtered and washed repeatedly with distilled water and ethanol, then dried at 60 °C for 10 h. Finally, the powder was calcined at 250 °C for 2 h in air to get NiO. NiO/Ni composites were synthesized by calcining the as prepared NiO at 190 °C in H_2 for 20 min, 40 min, and 60 min. They were denoted as NiO/Ni20, NiO/Ni40, and NiO/Ni60, respectively.

2.3 Characterization

The structures of the products were examined by X-ray power diffraction (XRD) on a Rigaku D/Max-2550 V diffractometer using $\text{Cu-K}\alpha$ radiation. The morphology of the products was observed on a transmission electron microscope (TEM Tecnai G20 FEI 200 KV) and a scanning electron microscope (SEM JEOL S-4800). The specific surface area was measured by the Brunauer–Emmett–Teller (BET) method at 77 K in a N_2 atmosphere using a Micromeritics ASAP 2010 surface area analyzer. Resistivity was tested by means of an Accent HL 5500 using thin, 5 mm diameter disks of powder, which were compacted mechanically at room temperature. The thickness of the thin disk was about 380 μm .

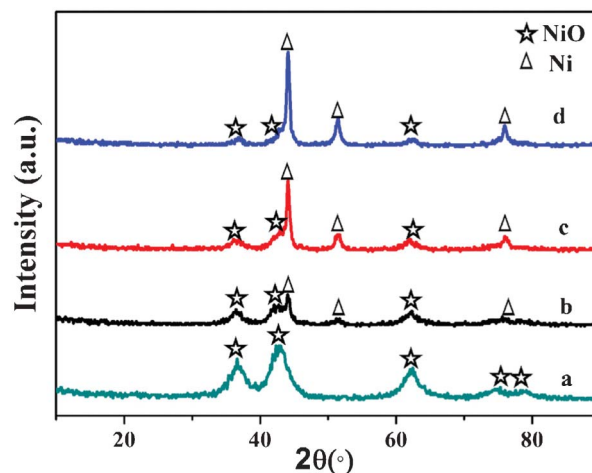


Fig. 1 XRD patterns of (a) NiO, (b) NiO/Ni20, (c) NiO/Ni40, (d) NiO/Ni60.

2.4 Electrochemical measurements

The working electrodes of supercapacitors were prepared by mixing the products, acetylene black and polytetrafluoroethylene (PTFE) binder (weight ratio of 70 : 20 : 10), this was then pressed onto a nickel foam current collector. Each working electrode contained about 3 mg of electrode material. All electrochemical measurements were done in a typical three-electrode system equipped with a working electrode, a platinum wire as the counter electrode, and Hg/HgO as the reference electrode. A 2 M aqueous solution of KOH was used as the electrolyte. Cyclic voltammetry (CV) was carried out on a Parstat 2273 electrochemical station (Princeton applied research CO., Ltd, USA). The galvanostatic charge and discharge tests were performed on a LAND CT2001A cell 50 measurement system. The specific capacitance was calculated based on the total mass of NiO and Ni.

3. Results and discussion

Fig. 1 shows the XRD image of NiO and the NiO/Ni composite. The phases of NiO (PDF#47-1049) and Ni (PDF#65-0380) are marked by “☆” and “△” respectively. As revealed in curve 1a, all the diffraction peaks can be indexed to NiO, which confirms NiO is pure phase. After reducing the NiO with H_2 , the peaks of Ni appear in the XRD patterns (curves 1b–d). In addition to the peaks from the NiO, other peaks can be assigned to Ni, demonstrating that the NiO/Ni composite has no other impurity phases. It can be noted that, with prolonged reduction time, the intensity of the Ni peaks increase, indicating the increase in the Ni component in the composites.

The morphology and the microstructure of NiO and the NiO/Ni composites were characterized by SEM (Fig. 2). It can be seen that pure NiO is bestrewn with many nanoflakelets with a thickness of about 10 nm, which form a hierarchical network-like structure (Fig. 2a). Fig. 2b–d shows the gradual changes of NiO/Ni from a flakelet to a particle-like morphology

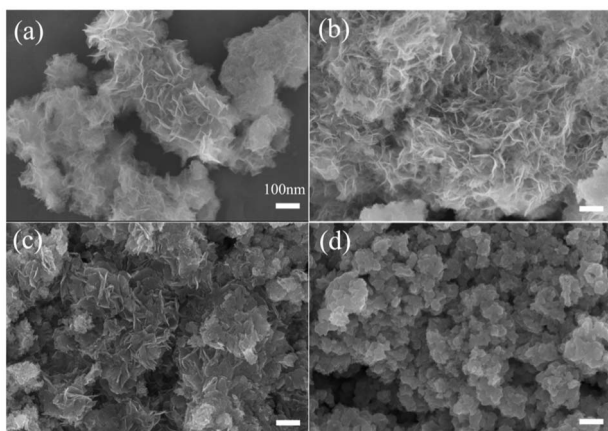


Fig. 2 SEM images of (a) NiO, (b) NiO/Ni20, (c) NiO/Ni40, (d) NiO/Ni60. The scale bar in all of the images is 100 nm.

with increasing reduction time. After reducing the NiO for 20 min, the composite NiO/Ni20 had a similar microstructure to NiO, with nanoflakelets dominating (Fig. 2b). When the reduction time is 40 min, some parts of the NiO/Ni40 collapsed and reunited into particles, still keeping the flakelet-like morphology generally (Fig. 2c). For the NiO/Ni60 composite, most of the flakelets changed into agglomerated larger particles and no flakelet-like structures can be observed clearly (Fig. 2d). In this process, time is the most significant controlling factor. With increasing reduction time, the reduction degree increases, and the destructiveness of morphology augments. Chemical titration revealed that the ratio of nickel elements in the composites increased gradually from 67.63% (NiO), to 68.48% (NiO/Ni20), to 76.57% (NiO/Ni40), to 80.76% (NiO/Ni60). It proves roughly that with the extension of reduction time, the amount of Ni increases, in good agreement with the results of the XRD. Moreover, the increment of the Ni component in the composites probably leads to the change in morphology.

Further research was carried out by TEM (Fig. 3). NiO has the flakelet-like units, demonstrating a thin hierarchical structure (Fig. 3a). The particles with a size distribution of 15–30 nm in the darker areas of the TEM images (Fig. 3 b–d) were confirmed to be Ni particles by EDS analysis. The darker areas of the TEM images increase gradually in NiO/Ni20, NiO/Ni40, and NiO/Ni60, suggesting an increase of Ni particles. The selected-area electron diffraction (SAED) patterns (inset), detected from the areas only covering collections of constituent nanoflakelets, show well-defined rings. They are indexed to the characteristic crystal planes of NiO and reveal their polycrystalline structure, in agreement with the XRD data. In NiO/Ni composites, NiO nanoflakelets serving as active materials have poor electrical conductivity, while Ni nanoparticles possess good electrical conductivity. As shown by TEM, Ni nanoparticles penetrate into the NiO nanoflakelets, so the NiO nanoflakelets with poor conductivity are connected through the Ni particles with high conductivity. Compared to the NiO nanoflakelets, the conductivity of the NiO/Ni

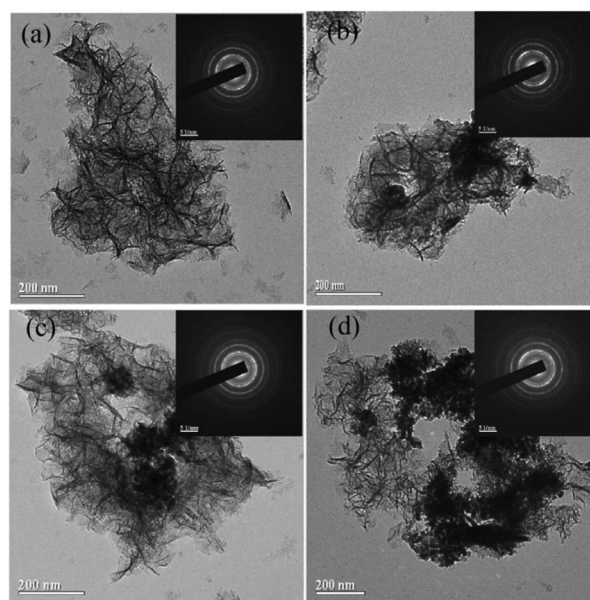


Fig. 3 TEM images of (a) NiO, (b) NiO/Ni20, (c) NiO/Ni40, (d) NiO/Ni60, (insets are SAED patterns).

composites is higher. And as the Ni component increases, the conductivity of the NiO/Ni composite augments. The conductive particles of Ni provide facile electron transport paths for fast Faradiac reaction and further improve availability of NiO.

In order to further characterize the structure of NiO and the NiO/Ni composites, nitrogen adsorption/desorption isotherms and the pore size distributions were measured (Fig. 4). With increasing reduction time, the BET specific surface areas decrease from 220.71 (NiO), to 205.81 (NiO/Ni20), to 137.25 (NiO/Ni40), and to 125.5 m² g⁻¹ (NiO/Ni60). This is reasonable since the agglomerated larger Ni particles show smaller specific surface areas than the NiO flakelets. The pore size

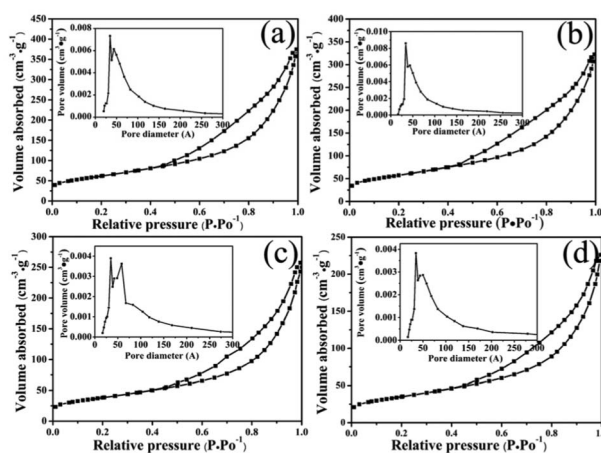


Fig. 4 Nitrogen adsorption-desorption isotherms (with the BJH pore size distribution plots in the insets) measured at 77 K for the (a) NiO, (b) NiO/Ni20, (c) NiO/Ni40, (d) NiO/Ni60.

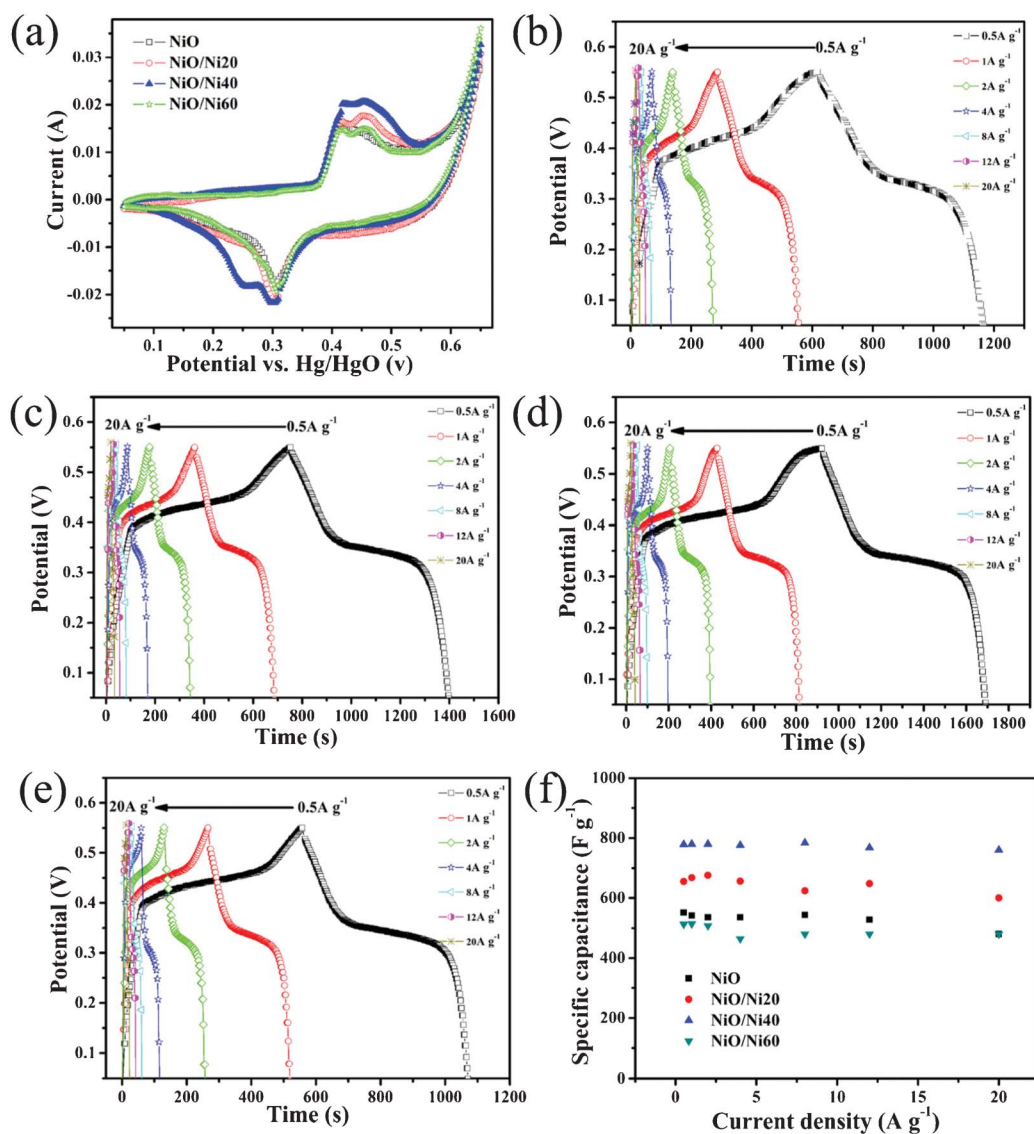


Fig. 5 Electrochemical characterizations of the NiO/Ni composites: (a) CV curves at a scan rate of 5 mV s⁻¹. Galvanostatic charge-discharge curves of NiO (b), NiO/Ni20 (c), NiO/Ni40 (d), and NiO/Ni60 (e) at various current densities. (f) Average specific capacitance at different current densities.

distribution plots given in the insets, state that the pore sizes of NiO and NiO/Ni are all 2–6 nm, calculated by the BJH method. The mesoporous structure is helpful to the performance of supercapacitors.^{36,37} The performance of NiO and NiO/Ni composites as electrode materials for supercapacitors was tested by cyclic voltammetry (CV). All the CV curves were measured by a three-electrode cell within a potential window of 0.05–0.65 V at a scan rate of 5 mV s⁻¹. As shown in Fig. 5a, the redox peaks correspond to the reversible reaction of Ni²⁺/Ni³⁺, which provides an active center for generating pseudocapacitance. The two redox peaks of the CV curves can be ascribed to the surface faradaic reactions related to Ni(OH)₂/NiOOH and NiO/NiOOH.³⁸ From the CV curves, it is calculated that, the specific capacitance firstly increases from 510 F g⁻¹ for NiO to 578 F g⁻¹ for NiO/Ni20 and to 641 F g⁻¹ for NiO/Ni40, then decrease to 480 F g⁻¹ for NiO/Ni60. Therefore, we

conclude that introducing an appropriate amount of Ni particles to the NiO can enhance the electrochemical performance of supercapacitors.

To discuss in detail, galvanostatic charge and discharge measurements were carried out to study the capacitance performance and rate performance of NiO and the NiO/Ni composites. The galvanostatic charge-discharge curves performed in a potential window of 0.05 V–0.55 V at different current densities are given in Fig. 5b–e, based on which the specific capacitances were calculated. As determined in Fig. 5f, NiO/Ni40 reveals a much better capacitance performance compared with the others at all current densities. The specific capacitance of NiO/Ni40 is calculated to be 779 F g⁻¹ at a current density of 0.5 A g⁻¹ based on the total mass of Ni and NiO. However, the value gradually decreases to 655, 552, and 513 F g⁻¹ for NiO/Ni20, NiO, and NiO/Ni60 respectively. It is

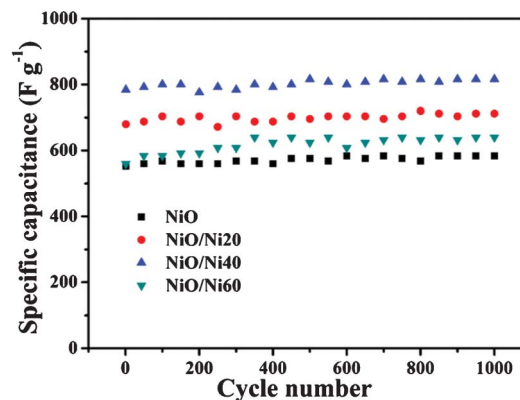
Table 1 Physical properties of the NiO/Ni systems

Samples	Specific surface area ($\text{m}^2 \text{g}^{-1}$)	BJH pore volume (cc g^{-1})	Resistivity (Ωm^{-2})
NiO	220	0.58	
NiO/Ni20	205	0.50	6.688×10^5
NiO/Ni40	137	0.40	2.459
NiO/Ni60	125	0.35	0.8829

worth while to note that the specific capacitance of NiO/Ni40 is 760 F g^{-1} at a high current density of 20 A g^{-1} , $\sim 98\%$ of that at 0.5 A g^{-1} . While for others, the corresponding values are 480, 600, and 480 F g^{-1} at 20 A g^{-1} for NiO, NiO/Ni20, and NiO/Ni60 respectively, with a capacitance retention of 87%, 92%, and 94% of that at 0.5 A g^{-1} . Apparently, the rate performance of NiO has been much improved after the introduction of Ni particles. Resistivity was also measured using thin disks of powder compacted mechanically. The sheet resistance (Table 1) gradually decreases from larger than $100 \text{ G}\Omega \text{ m}^{-2}$ for NiO to $6.688 \times 10^5 \text{ }\Omega \text{ m}^{-2}$ for NiO/Ni20, $2.459 \text{ }\Omega \text{ m}^{-2}$ for NiO/Ni40, and $0.8829 \text{ }\Omega \text{ m}^{-2}$ for NiO/Ni60. The conductivity of NiO/Ni40 and NiO/Ni60 is much closer and both are higher than NiO and NiO/Ni20.

For electrode materials, the morphology, weight ratio of active materials, and conductivity are generally crucial for the specific capacitance and rate performance. In this study, from NiO to NiO/Ni20 and NiO/Ni40, the morphology changes gradually, leading to a reduction in their specific surface areas. The weight ratio of NiO decreases gradually. Both of these factors are unfavorable for specific capacitance. However, their conductivities improve successively, which may enhance the specific capacitance greatly. The result of these three effects is that NiO/Ni40 shows optimal electrochemical performance. For NiO, NiO/Ni20 and NiO/Ni40, the specific capacitance increases gradually, as a result of the improved conductivity. For NiO/Ni40 and NiO/Ni60, their conductivities are both high. Yet, NiO/Ni60 has a lower specific surface area and content of NiO. Moreover, its morphology collapses seriously and reunites into particles. The agglomerated larger particles expose less surface area and pores than the flakelet-like structure, which makes it difficult for them to be in contact with the electrolyte and is disadvantageous for specific capacitance. Compared with conductivity, these two factors have a greater influence, leading to the lower specific capacitance of NiO/Ni60.

The stability of the capacitance performance of NiO and the NiO/Ni composites was evaluated by examination of the cycle performance at 4 A g^{-1} (Fig. 6). After the 1000-cycle test, the specific capacitance of NiO/Ni40 was still as high as 816 F g^{-1} . These results reveal that a high specific capacitance, remarkable rate performance and excellent cycle stability have been achieved in NiO/Ni40 supercapacitors.

**Fig. 6** Cyclic performance of the NiO/Ni systems at 4 A g^{-1} .

4. Conclusions

In summary, NiO/Ni composites, a mesoporous material of high electronic conductivity, have been prepared by a simple reduction method using H_2 . The weight ratio of NiO to Ni can be expediently adjusted by changing the reduction time. The different weight ratios of NiO to Ni has an effect on their performance as supercapacitor electrodes. Among the NiO/Ni composites, NiO/Ni40 exhibits the best performance because of its high conductivity and modest specific surface area. It achieves a high specific capacitance of 760 F g^{-1} at 20 A g^{-1} , suggesting a promising application as a supercapacitor electrode material. From this work, we open up a viewpoint that the introduction of Ni particles can enhance the conductivity of NiO as a supercapacitor electrode. This method can be extended to Co/Co₃O₄ or Fe/Fe₂O₃ composites as supercapacitors.

Acknowledgements

This work is supported by the National Basic Research Program of China (2012CB932303) and the National Natural Science Foundation of China (Grant No. 51072215 and 51172261).

References

- 1 S. Luo, K. Wang, J. P. Wang, K. L. Jiang, Q. Q. Li and S. S. Fan, *Adv. Mater.*, 2012, **24**, 2294–2298.
- 2 X. Wang, H. Guan, S. M. Chen, H. Q. Li, T. Y. Zhai, D. M. Tang, Y. Bando and D. Golberga, *Chem. Commun.*, 2011, **47**, 12280–12282.
- 3 J. P. Liu, J. Jiang, C. W. Cheng, H. X. Li, H. Gao and H. J. Fan, *Adv. Mater.*, 2011, **23**, 2076–2081.
- 4 J. T. Zhang, J. W. Jiang, H. L. Li and X. S. Zhao, *Energy Environ. Sci.*, 2011, **4**, 4009–4015.
- 5 S. Gu, R. Cai, T. Luo, Z. W. Chen, M. W. Sun, Y. Liu, G. H. He and Y. S. Yan, *Angew. Chem., Int. Ed.*, 2009, **48**, 6499–6502.

- 6 L. L. Zhang and X. S. Zhao, *Chem. Soc. Rev.*, 2009, **38**, 2520–2531.
- 7 K. Xie, X. T. Qin, X. Z. Wang, Y. N. Wang, H. S. Tao, Q. Wu, L. J. Yang and Z. Hu, *Adv. Mater.*, 2012, **24**, 347–352.
- 8 C. C. Hu, K. H. Chang, M. C. Lin and Y. T. Wu, *Nano Lett.*, 2006, **6**, 2690–2695.
- 9 C. Y. Cao, W. Guo, Z. M. Cui, W. G. Song and W. Cai, *J. Mater. Chem.*, 2011, **21**, 3204–3209.
- 10 Z. Y. Lu, Z. Chang, J. F. Liu and X. M. Sun, *Nano Res.*, 2011, **4**, 658–665.
- 11 M. W. Xu, S. J. Bao and H. L. Li, *J. Solid State Electrochem.*, 2007, **11**, 372–377.
- 12 X. Sun, G. K. Wang, J. Y. Hwang and J. Lian, *J. Mater. Chem.*, 2011, **21**, 16581–16588.
- 13 X. J. Zhang, W. H. Shi, J. X. Zhu, W. Y. Zhao, J. Ma, S. Mhaisalkar, T. L. Maria, Y. H. Yang, H. Zhang, H. H. Hng and Q. Y. Yan, *Nano Res.*, 2010, **3**, 643–652.
- 14 H. Jiang, T. Zhao, C. Z. Li and J. Ma, *J. Mater. Chem.*, 2011, **21**, 3818–3823.
- 15 H. L. Wang, H. S. Casalongue, Y. Y. Liang and H. J. Dai, *J. Am. Chem. Soc.*, 2010, **132**, 7472–7477.
- 16 Z. Y. Lu, Z. Chang, W. Zhu and X. M. Sun, *Chem. Commun.*, 2011, **47**, 9651–9653.
- 17 S. B. Yang, X. L. Wu, C. L. Chen, H. L. Dong, W. P. Hu and X. K. Wang, *Chem. Commun.*, 2012, **48**, 2773–2275.
- 18 R. B. Rakhi, W. Chen, D. Cha and H. N. Alshareef, *Nano Lett.*, 2012.
- 19 W. F. Wei, X. W. Cui, W. X. Chen and D. G. Ivey, *Chem. Soc. Rev.*, 2011, **40**, 1697–1721.
- 20 H. Lee, J. Kang, M. S. Cho, J. B. Choic and Y. Lee, *J. Mater. Chem.*, 2011, **21**, 18215–18219.
- 21 H. L. Wang, Q. M. Gao and L. Jiang, *Small*, 2011, **7**, 2454–2459.
- 22 J. R. Zhang, D. C. Jiang, B. Chen, J. J. Zhu, L. P. Jiang and H. Q. Fang, *J. Electrochem. Soc.*, 2001, **148**, 1362–1367.
- 23 Y. F. Yan, Q. L. Cheng, G. C. Wang and C. Z. Li, *J. Power Sources*, 2011, **196**, 7835–7840.
- 24 Y. Zhou, Z. Y. Qin, L. Li, Y. Zhang, Y. L. Wei, L. F. Wang and M. F. Zhu, *Electrochim. Acta*, 2010, **55**, 3904–3908.
- 25 S. W. Lee, J. Kim, S. Chen, P. T. Hammond and Y. Shao-Horn, *ACS Nano*, 2010, **4**, 3889–3896.
- 26 H. W. Wang, Z. A. Hu, Y. Q. Chang, Y. L. Chen, H. Y. Wu, Z. Y. Zhang and Y. Y. Yang, *J. Mater. Chem.*, 2011, **21**, 10504–10511.
- 27 X. Y. Lang, A. Hirata, T. Fujita and M. W. Chen, *Nat. Nanotechnol.*, 2011, **6**, 232–236.
- 28 Q. Lu, M. W. Lattanzi, Y. P. Chen, X. M. Kou, W. F. Li, X. Fan, K. M. Unruh, J. G. Chen and J. Q. Xiao, *Angew. Chem., Int. Ed.*, 2011, **50**, 1–5.
- 29 Z. Y. Lu, Z. Chang, W. Zhu and X. M. Sun, *Chem. Commun.*, 2011, **47**, 9651–9653.
- 30 G. X. Pan, X. Xia, F. Cao, P. S. Tang and H. F. Chen, *Electrochim. Acta*, 2012, **63**, 335–340.
- 31 M. Hasan, M. Jamal and K. M. Razeeb, *Electrochim. Acta*, 2012, **60**, 193–200.
- 32 M. Salari, S. H. Aboutalebi, K. Konstantinov and H. K. Liu, *Phys. Chem. Chem. Phys.*, 2011, **13**, 5038–5041.
- 33 J. Y. Kim, S. H. Lee, Y. Yan, J. Ohc and K. Zhu, *RSC Adv.*, 2012, **2**, 8281–8285.
- 34 M. Hasan, M. Jamal and K. M. Razeeb, *Electrochim. Acta*, 2012, **60**, 193–200.
- 35 J. Chang, J. Sun, C. H. Xu, H. Xu and L. Gao, *Nanoscale*, 2012, **4**, 6786–6791.
- 36 H. S. Zhou, D. L. Li, M. Hibino and I. Honma, *Angew. Chem., Int. Ed.*, 2005, **44**, 797–802.
- 37 T. Y. Wei, C. H. Chen, H. C. Chien, S. Y. Lu and C. C. Hu, *Adv. Mater.*, 2010, **22**, 347–351.
- 38 D. W. Wang, F. Li and H. M. Cheng, *J. Power Sources*, 2008, **185**, 1563–1568.